



## Characterization of MWCNTs-PMel Composite Film and Its Application in Simultaneous Determination of DOPA and Serotonin

Yogeswaran Umasankar,\* Ying Li, and Shen-Ming Chen\*\*z

Department of Chemical Engineering and Biotechnology, National Taipei University of Technology, Taipei 106, Taiwan

A composite film, which contains multiwalled carbon nanotubes (MWCNTs) incorporated with poly(melatonin) (PMel), has been synthesized on gold electrode by the potentiodynamic method. The presence of MWCNTs in the MWCNTs-PMel composite film enhances surface coverage concentration ( $\Gamma$ ) of PMel to  $\approx 640\%$  and increases the electron-transfer rate constant ( $k_s$ ) to  $\approx 17\%$ . The surface morphology of the MWCNTs-PMel composite film deposited on gold electrode has been studied using scanning electron microscopy and atomic force microscopy. These two techniques reveal that PMel is incorporated in MWCNTs. Electrochemical quartz crystal microbalance study reveals the enhancement in the functional properties of MWCNTs and PMel. The MWCNTs-PMel composite film exhibits enhanced electrocatalytic activity toward the biochemical compound mixture containing 3,4-dihydroxy-L-phenylalanine (DOPA) and serotonin. The electrocatalytic responses of these analytes at PMel, MWCNTs, and MWCNTs-PMel films were measured using cyclic voltammetry. From the electrocatalysis studies, well-separated voltammetric peaks have been obtained for DOPA and serotonin in MWCNTs-PMel composite film, with a peak separation of 145.1 mV. The sensitivity of MWCNTs-PMel composite film toward DOPA and serotonin is 0.4 and 0.22 mA mM<sup>-1</sup> cm<sup>-2</sup>, respectively. Similarly, the sensitivity of MWCNTs-PMel composite film toward DOPA and serotonin present in the mixture is 0.46 and 0.54 mA mM<sup>-1</sup> cm<sup>-2</sup>, respectively. These sensitivity values of MWCNTs-PMel composite film are higher than the PMel and MWCNT films.

© 2010 The Electrochemical Society. [DOI: 10.1149/1.3459907] All rights reserved.

Manuscript submitted March 16, 2010; revised manuscript received June 4, 2010. Published July 13, 2010.

3,4-Dihydroxy-L-phenylalanine (DOPA) is one of the naturally occurring amino acids in the human body produced from L-tyrosine. In the central nervous system, DOPA metabolizes to dopamine by aromatic L-amino acid decarboxylase. Similarly, serotonin is an important neurotransmitter in the central nervous system of mammals, which exists in the tissues and body fluids. Both DOPA and serotonin compounds control the functions of the nervous system and coexist in tissues and fluids.<sup>1-3</sup> Due to their crucial role in neurochemistry and industrial applications, several traditional methods have been used for their determination. Among these, the electrochemical method has more advantages over other methods because in this method the electrodes sense the neurotransmitters that are present in living organisms.<sup>4</sup> Electrochemical analysis at the unmodified electrodes has limitations because of the overlapping of oxidation potentials of biochemical compounds and hence often suffers from a pronounced fouling effect along with poor selectivity and reproducibility.<sup>5,6</sup> In the past, several modified electrodes were used for the simultaneous determination of neurotransmitters.<sup>7,8</sup> Among them, choline- and acetyl choline-modified electrodes have been used for the simultaneous measurement of dopamine, serotonin, and ascorbic acid.<sup>9</sup> However, there are no reported results for the simultaneous determination of DOPA and serotonin.

Electropolymerization is a simple but powerful method in targeting selective modification of different types of electrodes with desired matrices. However, the materials on the matrices do not possess peculiar properties when compared with those materials that are chemically synthesized by traditional methods. The electroactive polymers and carbon nanotube (CNT) matrices have received considerable attention in recent years. Numerous conjugated polymers have been electrochemically synthesized for their application in preparing chemical and biochemical sensor devices.<sup>10</sup> The conjugated polymers used in sensor devices exhibit enhancement in the electrocatalytic activity toward the oxidation and reduction of several biochemical and inorganic compounds,<sup>11</sup> where some of the functional groups in polymers act as catalysts.<sup>12-14</sup> In this paper, the phrase "enhanced electrocatalytic activity" could be explained as both an increase in peak current and a lower overpotential.<sup>15</sup> A wide variety

of matrices made of CNTs for the detection of inorganic and bio-organic compounds such as IO<sub>3</sub><sup>-</sup>, ascorbic acid, etc., has already been reported.<sup>16-18</sup>

Even though the electrocatalytic activity of conjugated polymers and CNT matrices individually shows good results, some properties such as mechanical stability, sensitivity for different techniques, and electrocatalysis for multiple compound detections are poor. To overcome this difficulty, new studies have been developed in the past decade for the preparation of composite films composed of both CNTs and conjugated polymers. The rolled-up graphene sheets of carbon exhibit a  $\pi$ -conjugative structure with a highly hydrophobic surface. This unique property of the CNTs allows them to interact with organic aromatic compounds through  $\pi$ - $\pi$  electronic and hydrophobic interaction to form new structures.<sup>19,20</sup> There are literatures available about the composite and sandwiched films prepared by polymer adsorption on CNTs. Some of these composite films have been used for electrocatalytic studies such as selective detection of dopamine in the presence of ascorbic acid.<sup>21</sup> Nanodevices have also been made by using these composite films.<sup>22</sup>

Among conjugated polymers, electrochemically synthesized biopolymers are widely used as the matrices for electrochemical determinations.<sup>23</sup> *N*-acetyl-5-methoxy tryptamine (melatonin) is one such biochemical compound used for the electrochemical synthesis of poly(melatonin) (PMel) biopolymer.<sup>24</sup> Briefly, in mammals, melatonin performs a diverse range of functions that include control of neuroendocrine events.<sup>25</sup> Melatonin is also known as an endogenous free radical scavenger.<sup>26,27</sup> It detoxifies a variety of free radicals, peroxy nitrite anion, singlet oxygen, etc.<sup>28</sup> Voltammetric investigation on the redox behavior of melatonin in the aqueous and non-aqueous solutions was already reported.<sup>29</sup> The literature survey reveals that there were no attempts made for the synthesis of composite film composed of CNTs and PMel. In this paper, we report about a novel composite film (MWCNTs-PMel) made of multiwalled carbon nanotubes (MWCNTs), which is incorporated with PMel biopolymer. The MWCNTs-PMel composite film's characterization, enhancement in functional properties, peak current, and electrocatalytic activity are also reported along with its application in the simultaneous determination of DOPA and serotonin. The film formation process involves the modification of a gold electrode with uniformly well-dispersed MWCNTs, which is then modified with PMel biopolymer.

\* Electrochemical Society Student Member.

\*\* Electrochemical Society Active Member.

<sup>z</sup> E-mail: smchen78@ms15.hinet.net

### Experimental

**Materials.**— Melatonin, MWCNTs (outer diameter = 10–20 nm, inner diameter = 2–10 nm, and length = 0.5–200  $\mu\text{m}$ ), DOPA, and serotonin bought from Aldrich and Sigma-Aldrich were used as received. All other chemicals used were of analytical grade. The preparation of aqueous solution was done with twice distilled deionized water. pH 7.0 phosphate buffer aqueous solution (PBS) was prepared from 0.1 M  $\text{Na}_2\text{HPO}_4$  and 0.1 M  $\text{NaH}_2\text{PO}_4$ . Solutions were deoxygenated by purging with prepurified nitrogen gas.

**Apparatus.**— Cyclic voltammetry (CV) was performed in an analytical system model CHI-1205 potentiostat. A conventional three-electrode cell assembly consisting of a Ag/AgCl reference electrode and a Pt wire counter electrode were used for the electrochemical measurements. The working electrode was either an unmodified gold electrode or a gold electrode modified with PMel, MWCNTs, or MWCNTs-PMel films; all the potentials were reported vs the Ag/AgCl reference electrode. The working electrode for electrochemical quartz crystal microbalance (EQCM) measurements was an 8 MHz AT-cut quartz crystal coated with a gold electrode. The diameter of the quartz crystal was 13.7 mm; the gold electrode diameter was 5 mm. Electrochemical impedance spectroscopy (EIS) measurements were performed using an IM6ex Zahner instrument (Kroanach, Germany). The morphological characterization of PMel, MWCNTs, and MWCNTs-PMel films was examined by means of a scanning electron microscope (SEM, Hitachi S-3000H) and an atomic force microscope (AFM, Being Nano-Instruments CSPM4000). All the measurements were carried out at 25°C ( $\pm 2$ ).

**Dispersion of MWCNTs and fabrication of MWCNTs-PMel film modified electrode.**— There was an important challenge in the preparation of MWCNTs. Because of its hydrophobic nature, it was difficult to disperse it in any aqueous solution to get a homogeneous mixture. Briefly, the hydrophobic nature of the MWCNTs was converted into a hydrophilic nature by following the previous studies.<sup>30</sup> This was done by weighing 10 mg of MWCNTs and 200 mg of potassium hydroxide into a ruby mortar and grinding them together for 2 h at room temperature. Then, the reaction mixture was dissolved in 10 mL of double distilled deionized water, and it was precipitated many times into methanol for the removal of potassium hydroxide. Thus, the obtained MWCNTs in 10 mL water were ultrasonicated for 6 h to get a uniform dispersion. This functionalization process of MWCNTs was done to get the hydrophilic nature, which was used to obtain the homogeneous dispersion of MWCNTs in water. This process not only converts MWCNTs to the hydrophilic nature but also helps to break down larger bundles of MWCNTs into smaller ones.

Before starting each experiment, gold electrodes were polished by a BAS polishing kit with 0.05  $\mu\text{m}$  alumina slurry, rinsed, and then ultrasonicated in double distilled deionized water. The gold electrodes studied were uniformly coated with 50  $\mu\text{g cm}^{-2}$  of MWCNTs and dried at  $\sim 40^\circ\text{C}$ . The electropolymerization of melatonin was done by electrochemical oxidation of melatonin (5 mM) on the MWCNT modified gold electrode using PBS. It was performed by consecutive CV over a suitable potential range of  $-0.3$  to  $0.55$  V; scan rate =  $100$   $\text{mV s}^{-1}$ . The optimization of PMel growth potential has been determined by various studies with different electropolymerization potentials (figures not shown). The obtained MWCNTs-PMel modified gold electrodes were washed carefully in deionized water to remove the melatonin present on the modified gold electrode and then dried at room temperature.

### Results and Discussion

**Preparation of PMel and MWCNTs-PMel composite films.**— The electropolymerization of melatonin (5 mM) using consecutive cyclic voltammograms on MWCNT modified gold electrode in PBS has been preformed for the preparation of MWCNTs-PMel composite film. Figure 1a and b represents the electropolymerization of

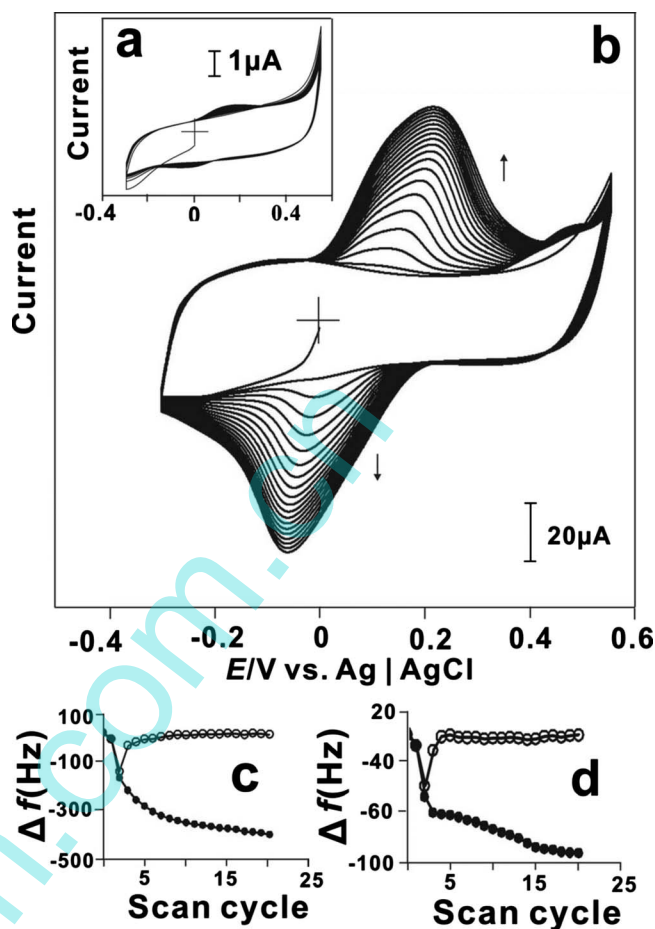


**Figure 1.** Repetitive CVs of (a) bare gold and (b) MWCNT coated gold electrodes modified from 5 mM melatonin present in PBS; scan rate  $100$   $\text{mV s}^{-1}$ . Consecutive potential CVs of a gold electrode modified with PMel at  $-0.3$  to  $0.55$  V (scan rate  $20$   $\text{mV s}^{-1}$ ), where (c) and (d) is the presence and absence of MWCNTs on the gold electrode, respectively. In both figures, frame circles and solid circles indicate every cycle frequency change with the increase in scan cycles and variation in frequency change with the increase in scan cycles, respectively.

melatonin on bare and MWCNT modified gold electrodes, respectively. The formal potentials of PMel redox peak at MWCNT modified and unmodified gold electrodes are at  $E^{0'} = 176.9$  and  $139.1$  mV vs Ag/AgCl, respectively. These formal potentials represent the redox reaction of PMel on the electrodes, whereas in the same figures, the oxidation of monomer occurred at  $493$  mV. On subsequent CV cycles, the redox peak current of PMel increases at both electrodes. This result indicates that during the CV cycle, the deposition of PMel takes place at both MWCNT modified and unmodified gold electrodes. Before transferring the film into PBS for other electrochemical characterizations, the prepared PMel and MWCNTs-PMel composite films have been washed carefully in deionized water to remove the melatonin present on the film. For initial electrochemical studies, the above prepared film modified gold electrodes (PMel and MWCNTs-PMel) have been characterized using simple CV techniques (figures not shown). The corresponding cyclic voltammograms have been measured at a  $20$   $\text{mV s}^{-1}$  scan rate in the potential range of  $-0.25$  to  $0.35$  V. In these experiments, too, the formal potentials of PMel redox couples in MWCNT modified and unmodified gold electrodes are at  $E^{0'} = 176.9$  and  $139.1$  mV vs Ag/AgCl, respectively.

The above CV results show that the presence of MWCNTs on the electrode has a catalytic effect on PMel deposition. These results are evident with the active surface coverage concentration ( $\Gamma$ ) of PMel

deposited at MWCNT modified ( $9.04 \text{ nmol cm}^{-2}$ ) and unmodified ( $0.01 \text{ nmol cm}^{-2}$ ) gold electrodes, where  $\Gamma$  of PMel is enhanced at the MWCNT film modified gold electrode when compared with the bare gold electrode.  $\Gamma$  of PMel has been calculated using the equation  $\Gamma = Q/nFA$ , where  $Q$  is the charge involved in the reaction,  $n$  is the number of electron transferred,  $F$  is Faraday's constant, and  $A$  is the geometric area of the electrode. The  $Q$  values have been calculated using the CHI software, and the geometric area of gold electrode is  $0.04 \text{ cm}^2$ . These  $\Gamma$  values show that MWCNTs enhance  $\Gamma$  of PMel by  $181 \text{ pmol cm}^{-2} \mu\text{g}^{-1}$ , and the overall increase in percentage of PMel  $\Gamma$  at MWCNT film is 640%. In these  $\Gamma$  calculations, the number of electrons involved in PMel redox reaction is assumed as two. The effective area of electrodes has also been calculated using the Randles-Sevcik equation, and the values are  $0.01 \text{ cm}^2$  for bare gold electrode,  $0.005 \text{ cm}^2$  for PMel,  $0.03 \text{ cm}^2$  for MWCNTs, and  $0.03 \text{ cm}^2$  for MWCNTs-PMel composite film modified gold electrodes. A detailed discussion about the relationship between the effective area of electrodes and their morphology is given in the topographic characterization of MWCNTs-PMel composite films using SEM and AFM section.

**EQCM studies of PMel and MWCNTs-PMel composite films.**—The EQCM experiments have been carried out by modifying the gold electrode of electrochemical quartz crystal by uniformly coating MWCNTs and then drying at  $40^\circ\text{C}$ . The increase in the voltammetric peak current of the PMel redox couple and the frequency decrease (or mass increase) are consistent with the growth of PMel film on MWCNT modified and unmodified gold electrodes (figures not shown). These results also show that the obvious deposition potential has started between  $-0.3$  and  $0.55 \text{ V}$ . From the frequency change, the change in the mass of PMel and MWCNTs-PMel composite films at the quartz crystal can be calculated by Sauerbrey (Eq. 1); however,  $1 \text{ Hz}$  frequency change is equivalent to  $1.4 \text{ ng cm}^{-2}$  of mass change.<sup>31,32</sup> The mass changes during PMel incorporation on MWCNT modified and unmodified gold electrodes for 20 cycles are  $0.67$  and  $0.13 \text{ } \mu\text{g cm}^{-2}$ , respectively. Similarly, from the voltammetric peak charge,  $\Gamma$  of PMel at MWCNT modified and unmodified gold electrodes at the 20th cycle shows  $0.5$  and  $0.08 \text{ nmol cm}^{-2}$ , respectively. From these  $\Gamma$  values and by considering PMel tetramer's molecular weight, the mass of PMel deposited on MWCNT modified and unmodified gold electrodes for 20 cycles have been calculated, and they are  $0.5$  and  $0.1 \text{ } \mu\text{g cm}^{-2}$ , respectively. These mass change values obtained from the  $\Gamma$  result are consistent with the mass change values obtained from the frequency change. The above mass and concentration values of PMel reveal that the deposition of PMel is higher at the MWCNT modified gold electrode than at the unmodified gold electrode.

$$\text{mass change}(\Delta m) = -\frac{1}{2}(f_0^{-2})(\Delta f)A(K\rho)^{1/2} \quad [1]$$

where  $f_0$  is the oscillation frequency of the crystal,  $\Delta f$  is the frequency change,  $A$  is the area of gold disk,  $K$  is the shear modulus of the crystal, and  $\rho$  is the density of the crystal. Figure 1c and d shows the scan cycles vs frequency change plots of the PMel deposition at the MWCNT modified and unmodified gold electrodes, respectively. In these figures, the solid circle plots show the gross change in the peak current and frequency shifts over the course of the experiment, which are consistent. Similarly, the frame circle plots show the change between consecutive scans  $\Delta f_n - \Delta f_{n-1}$ , which clearly reveals that the peak current and  $\Delta f$  change at a constant rate during consecutive scans after few cycles. These EQCM results show that the deposition of PMel on the MWCNT film is more stabilized and more homogeneous than on the bare gold electrode.

**EIS studies of PMel, MWCNTs, and MWCNTs-PMel composite films.**—Figure 2a shows the impedance spectra represented as Nyquist plots ( $Z_{\text{im}}$  vs  $Z_{\text{re}}$ ) for bare gold electrode, PMel, MWCNTs, and MWCNTs-PMel composite films on gold electrode using  $5 \text{ mM Fe}(\text{CN})_6^{3-/4-}$ . Figure 2b shows the same bare gold electrode,

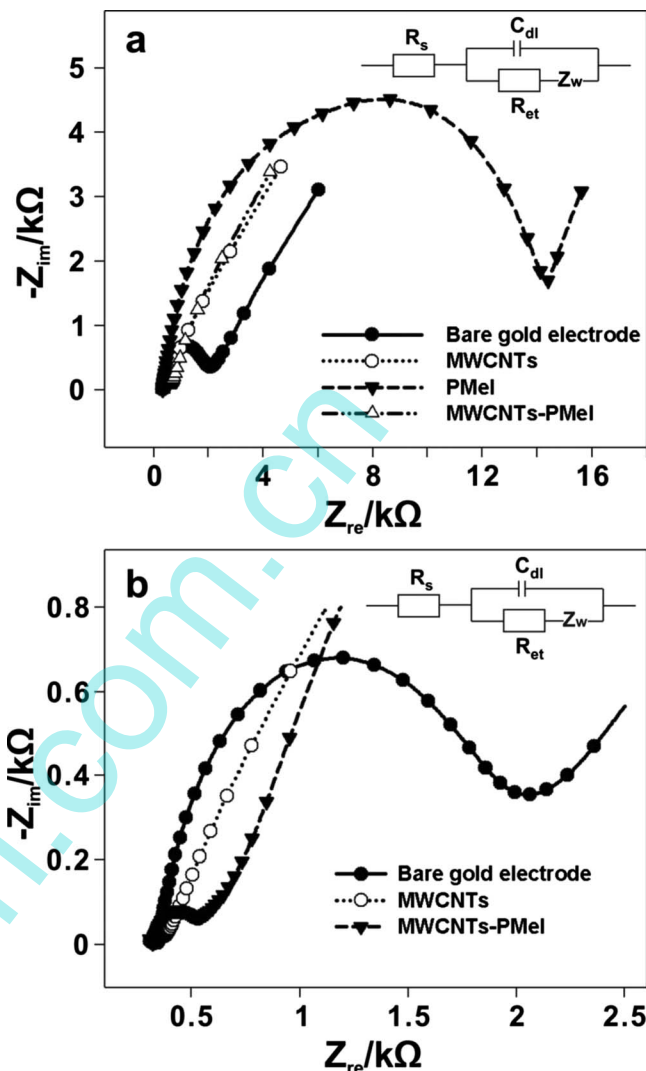


**Figure 2.** (a) EIS of bare gold, PMel, MWCNTs, and MWCNTs-PMel modified gold electrodes in  $5 \text{ mM Fe}(\text{CN})_6^{3-}/\text{Fe}(\text{CN})_6^{4-}$  in PBS. Amplitude:  $5 \text{ mV}$ , frequency:  $0.01 \text{ Hz}$  to  $1000 \text{ kHz}$ . (b) EIS of bare gold, MWCNTs, and MWCNTs-PMel modified gold electrodes at similar conditions. Insets in (a) and (b) show the Randles circuit for the above mentioned electrodes.

MWCNTs, and MWCNTs-PMel composite films in magnified scale. Insets of Fig. 2a and b represent the Randles equivalent circuit model used for fitting the experimental data, where  $R_s$  is the electrolyte resistance,  $R_{\text{et}}$  is the charge transfer resistance,  $C_{\text{dl}}$  is the double layer capacitance, and  $Z_w$  is the Warburg impedance. The semicircle which appeared in the Nyquist plots indicates the parallel combination of charge-transfer resistance and double layer capacitance, resulting from electrode impedance.<sup>33</sup> All the above mentioned films exhibit semicircles with various diameters in the frequency range  $0.01 \text{ Hz}$ – $1000 \text{ kHz}$ . The semicircles obtained at a lower frequency correspond to a diffusion limited electron-transfer process and at a higher frequency represent a charge-transfer limited process. The EIS results show that the area of semicircle for the PMel film is greater than that of the bare gold electrode, which is greater than that of the MWCNTs-PMel composite film. However, the MWCNT film's semicircle is smaller than the MWCNTs-PMel composite film. To find the electron-transfer efficiency of the electrodes,  $R_{\text{et}}$  values have been obtained for each one of the modified and unmodified electrodes by fitting the above Nyquist plot results with the Randles equivalent circuit model. The obtained  $R_{\text{et}}$  values of bare gold electrode, PMel, MWCNTs, and MWCNTs-PMel com-

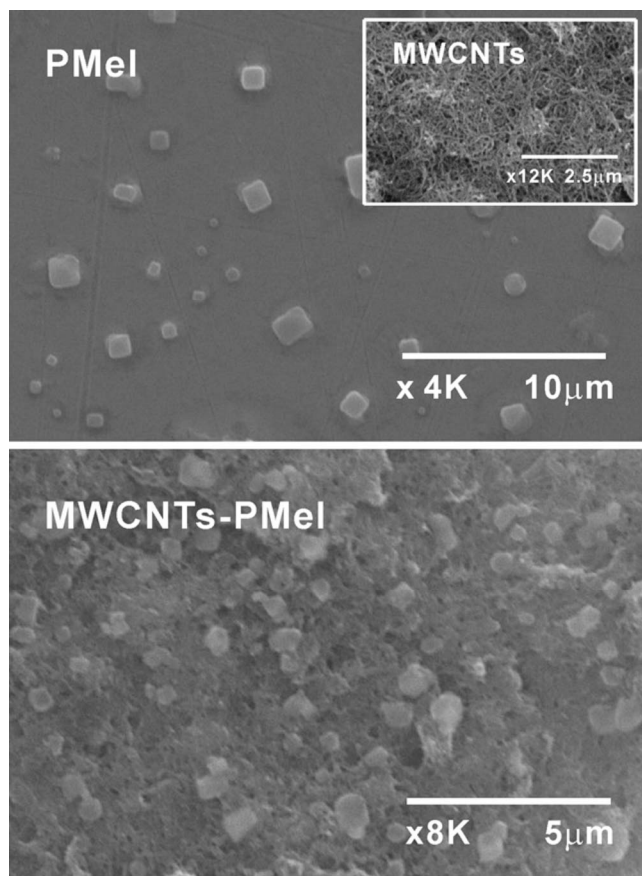


**Figure 3.** SEM images of PMel, MWCNTs, and MWCNTs-PMel films.

posite films are 151.7, 717.6, 1075.7, and 5816.7  $\Omega \text{ cm}^{-2}$ , respectively, where the area represents the effective area of respective electrodes. The above values reveal that the charge-transfer resistance for MWCNTs-PMel composite film is lower than the PMel film and bare gold electrode but greater than the MWCNT film. This proves that MWCNTs present in the MWCNTs-PMel composite film enhances electron shuttling between PMel and the electrode surface.

*Topographic characterization of MWCNTs-PMel composite film using SEM and AFM.*—PMel, MWCNTs, and MWCNTs-PMel composite films have been prepared on gold electrode with similar conditions and similar potentials as mentioned in the previous sections and were characterized using SEM. The prolonged exposure to electron beam damages the PMel biopolymer present in the above mentioned films, so utmost care has been taken to measure these images. A comparison of SEM images in Fig. 3 reveals significant morphological differences among PMel, MWCNT, and MWCNTs-PMel films. The top views of the microstructures of PMel on the bare gold electrode surface in Fig. 3 show cubes of PMel deposited on the electrode. A comparison of PMel with MWCNTs-PMel film reveals that PMel cubes deposited on MWCNTs are smaller and more numerous than PMel deposited on bare electrode. Similarly, bare gold electrode (figure not shown) and only MWCNT film have also been measured, which shows a uniform deposition of MWCNTs on the gold surface. The PMel, MWCNTs, and MWCNTs-PMel composite film modified gold electrodes have also been used to measure AFM topography images shown in Fig. 4. The higher magnification ( $10 \times 10 \mu\text{m}$ ) of AFM images when compared with the SEM images reveals that PMel cubes are not in perfect symmetry. Similar to the SEM images, AFM results also show that a denser deposition of PMel takes places in the presence of MWCNTs. This result is consistent with  $\Gamma$  values and EQCM results given in the above sections. The thicknesses of PMel, MWCNTs, and MWCNTs-PMel have been obtained from AFM results, which are 160, 348, and 348 nm, respectively. These values, along with the morphological structures, show that when compared with the PMel film, the MWCNTs and MWCNTs-PMel films have more materials with a high surface area on the electrode surface. This observation is consistent with the effective area of the electrodes calculated in the previous section, where the effective area is higher for MWCNTs and MWCNTs-PMel films than for PMel film. The thickness values also show that MWCNTs-PMel is thicker than PMel, which is due to the presence of MWCNTs. These SEM and AFM results reveal the coexistence of PMel and MWCNTs in the MWCNTs-PMel composite film.

*Electrochemical studies of MWCNTs-PMel composite film.*—The cyclic voltammograms of MWCNTs-PMel composite film in PBS at different scan rates show that the anodic and cathodic peak currents of the composite film's redox couple increase linearly with the increase in scan rates (figure not shown). The ratio of  $I_{pa}/I_{pc}$  demonstrates that the redox process is not controlled by diffusion. However, the  $\Delta E_p$  of each scan rate reveals that the peak separation

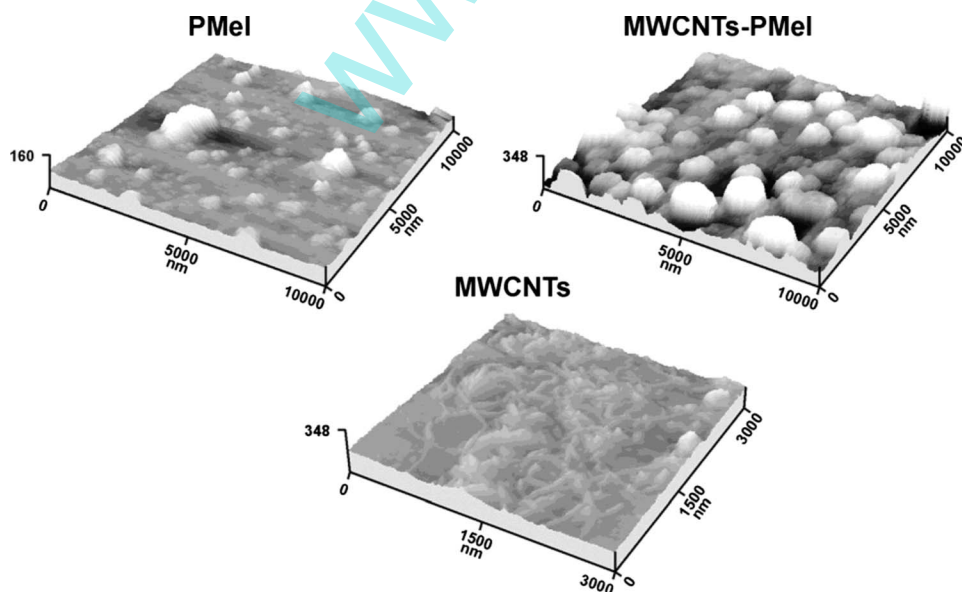


**Figure 4.** AFM images of PMel, MWCNTs, and MWCNTs-PMel films.

of the composite's redox couple increases as the scan rate increases (figure not shown). From the slope values of  $\Delta E$  vs  $\log$  scan rate, by assuming the value of  $\alpha \approx 0.5$ , number of electrons involved as two, the electron-transfer rate constant ( $k_s$ ) has been calculated using Eq. 2 based on the Laviron theory.<sup>34</sup> The  $k_s$  values are 0.14 and 0.17  $s^{-1}$  for PMel and MWCNTs-PMel film-modified gold electrodes, respectively. From these  $k_s$  values, the increase in the ability of electron transfer between the electrode surface and PMel in the presence of MWCNTs have been calculated, and it is  $\approx 17\%$ . This result is similar to the EIS results given in the EIS studies of PMel, MWCNTs, and MWCNTs-PMel composite films section, where the presence of MWCNTs decreases the electron-transfer resistance of the composite film. In Eq. 2, the scan rate and  $\Delta E$  values are in unit volts

$$\log k_s = \alpha \log(1 - \alpha) + (1 - \alpha) \log \alpha - \log(RT/nFv) - \alpha(1 - \alpha)nF\Delta E/2.3RT \quad [2]$$

The MWCNTs-PMel composite film modified gold electrode has been studied at various pH aqueous solutions. The MWCNTs-PMel on gold electrode has been obtained in PBS, washed with deionized water, and transferred to various pH aqueous buffer solutions for CV studies without the presence of melatonin. The results show that the film is highly stable in the pH range between 1 and 13 (figures not shown). The values of  $E_{pa}$  and  $E_{pc}$  depend on the pH value of buffer solution. The plot of peak potential of MWCNTs-PMel over the pH range from 1 to 13 shows the response of  $-57 \text{ mV pH}^{-1}$ , which is close to that given by the Nernstian equation for equal number of electron and proton transfer. All the above results show the enhanced functional properties of the MWCNTs-PMel composite film in the presence of both PMel and MWCNTs.

#### Electrocatalysis of DOPA and serotonin individually at PMel, MWCNTs, and MWCNTs-PMel film modified gold electrodes.—

The electrochemical oxidation of DOPA and serotonin at different film modified gold electrodes has been carried out using PBS at 20  $\text{mV s}^{-1}$  in the potential range of  $-0.25$  to  $0.35 \text{ V}$ , as given in Fig. 5a and b, respectively. The different electrodes used are bare gold electrode, PMel, MWCNTs, and MWCNTs-PMel composite film modified gold electrodes. All the cyclic voltammograms have been recorded at the constant time interval of 2 min with nitrogen purging before the start of each experiment. The cyclic voltammogram for the MWCNTs-PMel film exhibits a redox couple in the absence of analytes, whereas there is no redox peak for the MWCNT film. In the presence of DOPA or serotonin, the oxidation peak of the respective analytes appears at the  $E_{pa}$  values, which is given in Table I for both MWCNTs and MWCNTs-PMel films. No peak appears at the bare gold electrode and PMel film for both DOPA and serotonin. From these  $E_{pa}$  values in Table I, it is obvious that the DOPA's peak current appears at a lower positive potential than serotonin. An increase in the concentration of DOPA or serotonin simultaneously produces a linear increase in the oxidation peak currents of the respective analytes at MWCNTs and MWCNTs-PMel films, as shown in the inset plots of Fig. 5a and b, respectively. The current response with linear concentration range for both analytes almost covers the concentration range found in the physiological conditions. From the slopes of the linear calibration curves, the sensitivity and the correlation coefficients of MWCNTs and MWCNTs-PMel film modified gold electrodes toward the analytes have been calculated and are given in Table I. These values and the  $I_{pa}$  values in the same table show that the peak current of both analytes are high at the MWCNTs-PMel composite film compared with the MWCNT film. The above results reveal that the enhanced electrocatalysis of both analytes takes place at the MWCNTs-PMel film than at the MWCNT film, where the increase in current and decrease in overpotential are both considered as the enhancement of electrocatalysis.<sup>15</sup>

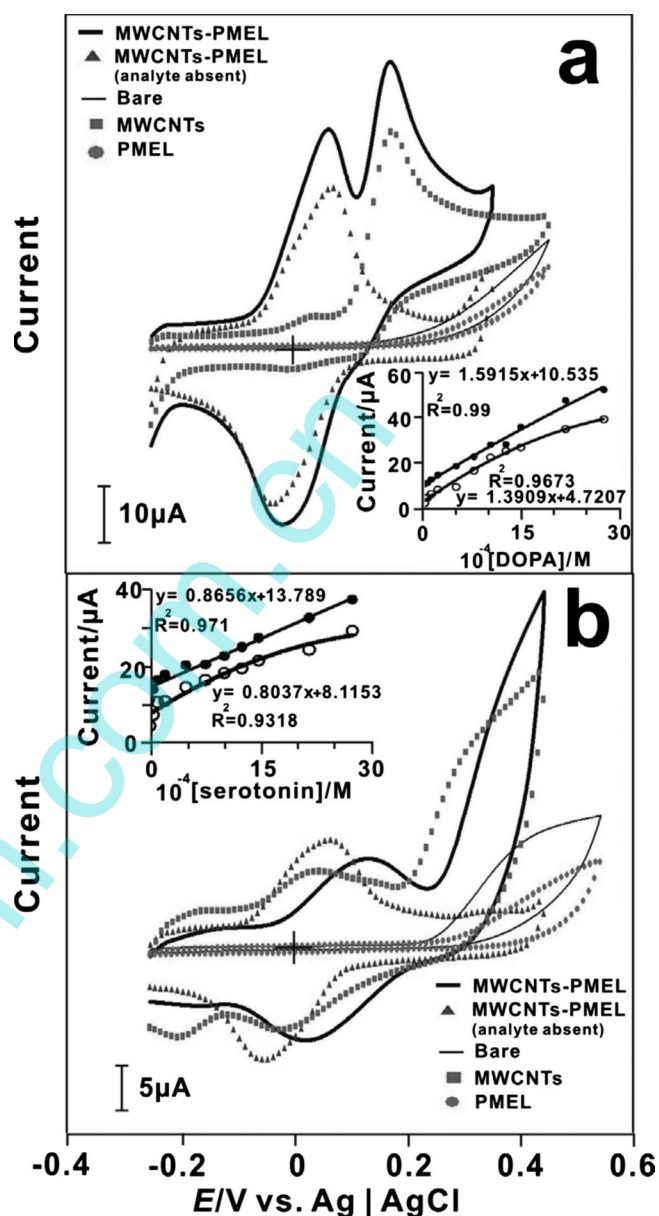


**Figure 5.** CVs of (a) DOPA and (b) serotonin at various electrodes using PBS at 20  $\text{mV s}^{-1}$ ; where in both figures, MWCNTs-PMel is shown with and without the presence of analytes. Similarly, bare gold electrode, PMel, and MWCNT modified gold electrodes are shown in the presence of the highest concentration of analytes. The concentration ranges of analytes are given in Table I. The insets in both figures are the plots of peak current vs concentration of analytes at MWCNT (frame circles) and MWCNTs-PMel (solid circles) films.

*Voltammetric resolution of analytes present in the mixture at PMel, MWCNTs, and MWCNTs-PMel film modified gold electrodes.—* Figure 6 shows the electrochemical oxidation cyclic voltammograms that have been obtained for DOPA and serotonin coexisting (1:1 analyte mixture) at PMel, MWCNT, and MWCNTs-PMel films using PBS at 20  $\text{mV s}^{-1}$  in the potential range of  $-0.25$  to  $0.45 \text{ V}$ , where the MWCNTs-PMel film is given in the presence and absence of the analyte mixture. The bare gold electrode, PMel, and MWCNT films are given at the highest concentration of the analyte mixture. The lowest and highest concentrations of the analyte mixture are given in Table I. The cyclic voltammograms of bare gold electrode in Fig. 6 exhibit only one broad peak; here the broad peak represents the voltammetric signals of the analyte mixture.

**Table I.** Electroanalytical result for DOPA and serotonin individually and in mixture at various modified gold electrodes using CV techniques in PBS.

Analytes	Epa (mV)	Ipa ( $\mu\text{A}$ )	Concentration range (mM)		Sensitivity ( $\text{mA mM}^{-1} \text{cm}^{-2}$ ) <sup>c</sup>		
			Low	High			
Individual	DOPA	<sup>a</sup>	174	39	0.19	27.1	0.35 [0.9673]
		<sup>b</sup>	170	52	0.19	27.1	0.4 [0.9900]
	Serotonin	<sup>a</sup>	341	29	0.19	27.1	0.2 [0.9318]
		<sup>b</sup>	392	37	0.19	27.1	0.22 [0.9710]
Mixture	DOPA	<sup>a</sup>	181	22	0.19	40.2	0.13 [0.9250]
		<sup>b</sup>	249	84	0.19	40.2	0.46 [0.9888]
	Serotonin	<sup>a</sup>	336	37	0.19	40.2	0.22 [0.9611]
		<sup>b</sup>	394	93	0.19	40.2	0.54 [0.9862]

<sup>a</sup> MWCNT modified gold electrode.<sup>b</sup> MWCNTs-PMel modified gold electrode.<sup>c</sup> The correlation coefficients are given in parentheses.

Moreover, the peak current decreases in the subsequent cycles for both PMel film and bare gold electrode. These observations indicate that both PMel film and bare gold electrode fail to separate the voltammetric signals of analytes in the mixture. The fouling effect of the electrode surface with the oxidized products of analytes is the reason for obtaining the weak single peak for analytes in the mixture.<sup>35</sup> The cyclic voltammogram for MWCNTs-PMel film exhibits a redox couple in the absence of the analyte mixture. In the presence of the analyte mixture, new growth in the oxidation peaks of respective analytes appears at the Epa values, which are given in Table I for both MWCNT and MWCNTs-PMel films. From these Epa values, the peak separation between DOPA and serotonin at MWCNT and MWCNTs-PMel composite films has been calculated,

which are 154.2 and 145.1 mV, respectively. An increase in concentration of the analyte mixture simultaneously produces a linear increase in the oxidation peak currents of both analytes with good film stability, as shown in the inset of Fig. 6.

The Ipa values from Table I show that the anodic peak current of both analytes at MWCNTs-PMel film is higher than at MWCNT film, which reveals that PMel's redox reaction involves and enhances the peak current of analytes. In these results, the increase in current and decrease in potential are both considered as the enhancement of electrocatalysis.<sup>15</sup> From the slopes of the linear calibration curves (Fig. 6 inset), sensitivity of the MWCNT and MWCNTs-PMel film-modified gold electrodes and their correlation coefficients have been calculated and given in Table I. In these results, too, the sensitivity of MWCNTs-PMel is higher than MWCNTs for both the analytes. Apart from the 1:1 DOPA and serotonin mixture ratio, various mixture ratios at the MWCNTs-PMel film have been studied. The sensitivity values for DOPA at the MWCNTs-PMel film are 0.36, 0.42, 0.38, and 0.39  $\text{mA mM}^{-1} \text{cm}^{-2}$  for 1:4, 1:6, 4:1, and 6:1 (DOPA:serotonin), respectively. Similarly, the sensitivity values for serotonin at the MWCNTs-PMel film are 0.48, 0.46, 0.51, and 0.45  $\text{mA mM}^{-1} \text{cm}^{-2}$  for 1:4, 1:6, 4:1, and 6:1 (DOPA:serotonin), respectively. When comparing the above values, Table I shows that there is not much difference in sensitivity values even if the concentration of DOPA or serotonin present in the mixture varied widely.

A quantitative analysis of DOPA and serotonin in the mixture has been carried out with the help of interference studies, where the interference of serotonin on DOPA and the interference of DOPA on serotonin have been studied in detail. The experiments include the study of change in peak current (for 4.02 mM) of either of the analytes by varying the concentration of one. The result shows that serotonin does not interfere with DOPA's peak current up to 0.5 mM. However, concentrations higher than 0.5 mM decrease the peak current of DOPA at the rate of 1.3  $\mu\text{A mM}^{-1}$  of serotonin. Similarly, the peak current of serotonin does not change up to 0.2 mM of DOPA, whereas concentrations higher than 0.2 mM increase the peak current of serotonin at the rate of 3.5  $\mu\text{A mM}^{-1}$  of DOPA. Using the above interference values, the real Ipa for DOPA and serotonin at 4.02 mM in the 1:1 mixture have been calculated from Table I, and they are 89 and 79  $\mu\text{A}$ , respectively. From all the above results, it is obvious that MWCNTs-PMel composite film is efficient for the simultaneous determination of DOPA and serotonin present in the mixture.

## Conclusions

A novel composite material has been developed using MWCNTs and PMel at a gold electrode, which is stable in PBS. The developed MWCNTs-PMel composite film combines the advantages of ease of fabrication, high reproducibility, and sufficient long-term stability.

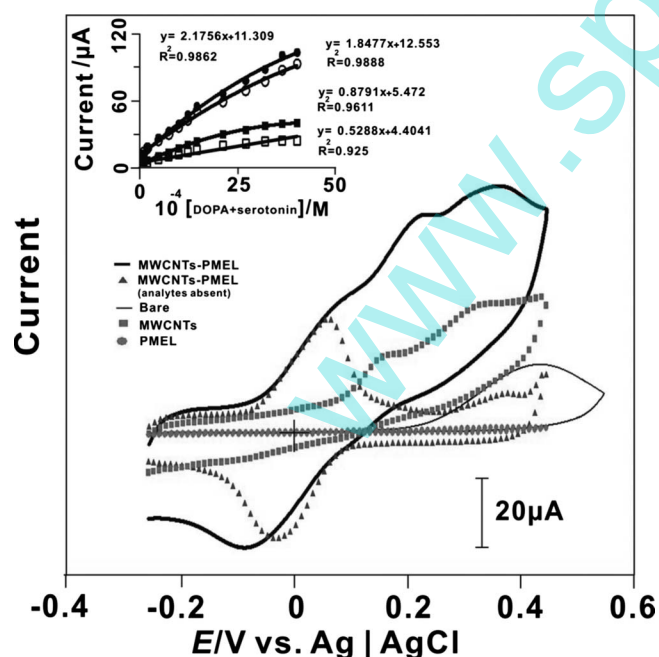


**Figure 6.** CVs of DOPA and serotonin present in analyte mixture (1:1) at various electrodes using PBS at 20  $\text{mV s}^{-1}$ ; where, MWCNTs-PMel is shown with and without the presence of analytes. Similarly, bare gold electrode, PMel and MWCNT modified gold electrodes are shown in the presence of the highest concentration of analyte mixture. The concentration ranges of analytes present in the mixture are given in Table I. The inset is the plot of peak current vs concentration of DOPA at MWCNTs (frame square) and MWCNTs-PMel (frame circle), serotonin at MWCNT (solid square), and MWCNTs-PMel (solid circle) films.

The experimental method of CV with a composite film biosensor integrated into the gold electrode presented in this paper provides an opportunity for qualitative and quantitative characterization and simultaneous determination of DOPA and serotonin. Further, MWCNTs-PMel composite film has excellent catalytic activity on DOPA and serotonin. Therefore, this work establishes and illustrates, in principle and potential, a simple and novel approach for the development of a simultaneous DOPA and serotonin voltammetric sensor based on modified gold electrode.

#### Acknowledgment

This work was supported by the National Science Council and the Ministry of Education of Taiwan.

National Taipei University of Technology assisted in meeting the publication costs of this article.

#### References

1. M. Oksman, H. Tanila, and L. Yavich, *Neuropharmacology*, **56**, 647 (2009).
2. X. Borue, S. Cooper, J. Hirsh, B. Condrion, and B. J. Venton, *J. Neurosci. Methods*, **179**, 300 (2009).
3. D. L. Murphy, A. Lerner, G. Rudnick, and K. P. Lesch, *Mol. Interv.*, **4**, 109 (2004).
4. B. J. Venton and R. M. Wightman, *Anal. Chem.*, **75**, 414A (2003).
5. J. Chen and C. S. Cha, *J. Electroanal. Chem.*, **463**, 93 (1999).
6. M. A. Dayton, A. G. Ewing, and R. M. Wightman, *Anal. Chem.*, **52**, 2392 (1980).
7. Z. Yang, G. Hu, X. Chen, J. Zhao, and G. Zhao, *Colloids Surf., B*, **54**, 230 (2007).
8. P. Ramesh, G. S. Suresh, and S. Sampath, *J. Electroanal. Chem.*, **561**, 173 (2004).
9. G. P. Jin, X. Q. Lin, and J.-M. Gong, *J. Electroanal. Chem.*, **569**, 135 (2004).
10. C. P. McMahon, G. Rocchitta, S. M. Kirwan, S. J. Killoran, P. A. Serra, J. P. Lowry, and R. D. O'Neill, *Biosens. Bioelectron.*, **22**, 1466 (2007).
11. I. Becerik and F. Kadirgan, *Synth. Met.*, **124**, 379 (2001).
12. T. Selvaraju and R. R. Ramaraj, *J. Electroanal. Chem.*, **585**, 290 (2005).
13. M. Mao, D. Zhang, T. Sotomura, K. Nakatsu, N. Koshiba, and T. Ohsaka, *Electrochim. Acta*, **48**, 1015 (2003).
14. M. Yasuzawa and A. Kunugi, *Electrochem. Commun.*, **1**, 459 (1999).
15. C. P. Andrieux, O. Haas, and J. M. SavGant, *J. Am. Chem. Soc.*, **108**, 8175 (1986).
16. J. Wang and M. Musameh, *Anal. Chim. Acta*, **511**, 33 (2004).
17. H. Cai, X. Cao, Y. Jiang, P. He, and Y. Fang, *Anal. Bioanal. Chem.*, **375**, 287 (2003).
18. A. Erdem, P. Papakonstantinou, and H. Murphy, *Anal. Chem.*, **78**, 6656 (2006).
19. Q. Li, J. Zhang, H. Yan, M. He, and Z. Liu, *Carbon*, **42**, 287 (2004).
20. J. Zhang, J. K. Lee, Y. Wu, and R. W. Murray, *Nano Lett.*, **3**, 403 (2003).
21. M. Zhang, K. Gong, H. Zhang, and L. Mao, *Biosens. Bioelectron.*, **20**, 1270 (2005).
22. R. J. Chen, Y. Zhang, D. Wang, and H. Dai, *J. Am. Chem. Soc.*, **123**, 3838 (2001).
23. Y. Li, Y. Umasankar, and S.-M. Chen, *Anal. Biochem.*, **388**, 288 (2009).
24. V. S. Vasantha and S.-M. Chen, *J. Electrochem. Soc.*, **152**, D151 (2005).
25. R. J. Reiter, *Endocr. Rev.*, **12**, 151 (1991).
26. D.-X. Tan, L.-D. Chen, B. Poeggeler, L. C. Manchester, and R. J. Reiter, *Endocr. J.*, **1**, 57 (1993).
27. D.-X. Tan, L. C. Manchester, R. J. Reiter, B. F. Plummer, L. J. Hardies, S. T. Weintraub, B. Vijayalaxmi, and A. M. M. Shepherd, *Biochem. Biophys. Res. Commun.*, **253**, 614 (1998).
28. R. J. Reiter, D.-X. Tan, J. Cabrera, D. D'Arpa, R. M. Sainz, J. C. Mayo, and S. Ramos, *Biol. Signals Recept.*, **8**, 56 (1999).
29. A. Radi and G. E. Bekhiet, *Bioelectrochem. Bioenerg.*, **45**, 275 (1998).
30. Y. Yan, M. Zhang, K. Gong, L. Su, Z. Guo, and L. Mao, *Chem. Mater.*, **17**, 3457 (2005).
31. S. M. Chen, C. J. Liao, and V. S. Vasantha, *J. Electroanal. Chem.*, **589**, 15 (2006).
32. S. M. Chen and M. I. Liu, *Electrochim. Acta*, **51**, 4744 (2006).
33. H. O. Finklea, D. A. Snider, and J. Fedyk, *Langmuir*, **9**, 3660 (1993).
34. E. Laviron, *J. Electroanal. Chem.*, **101**, 19 (1979).
35. C. R. Raj, K. Tokuda, and T. Ohsaka, *Bioelectrochemistry*, **53**, 183 (2001).